J. Fluid Mech. (1994), *vol.* 276, *pp.* 113–124

The offshore vortex train

By N. MATSUNAGA[1], K. TAKEHARA[2] AND Y. AWAYA[3]

[1] Department of Earth System Science and Technology, Kyushu University, Kasuga-shi 816, Japan

[2] Department of Civil Engineering, Kinki University, Osaka 577, Japan

[3] Department of Land and Water Development, Kyushu-Kyoritsu University, Kitakyushu-shi 807, Japan

(Received 28 September 1992 and in revised form 20 October 1993)

A row of two-dimensional vortices forms in an offshore zone when regular surface waves run up a sloping flat bed. This vortex row is called the offshore vortex train. The vortices begin to appear near the breaking point. Moving in the offshore direction, they develop and increase their horizontal lengthscale through vortex merging. After reaching a particular offshore location, however, they decay rapidly. The formation region of the vortex train has been investigated on the basis of visual experiments for three bed slopes. Its formation does not depend on the type of wave breaking but is observed when the steepness of deep-water waves is smaller than 4.2×10^{-2}. The horizontal lengthscale of the vortices and the velocities of the vortex movement have also been evaluated empirically.

1. Introduction

Coastal regions have attracted considerable research attention because of the central role which they play in the budget of sediment, the generation of nearshore currents, the diffusion of pollutant, etc. Such regions are usually divided into the nearshore zone and the offshore zone (e.g. Komar 1976). Typical features of the nearshore zone are breaking waves and turbulent fluid motion. Miller (1976) described the formation of breaker vortices from the behaviour of air bubbles entrained due to wave breaking. Since his work, the turbulence structure in this zone has been investigated vigorously through field observations and laboratory experiments. Most of these studies, which have been reviewed in detail by Peregrine (1983) and Battjes (1988), are mainly concerned with coherent structures near the free surface. Matsunaga & Honji (1980) and Matsunaga, Takehara & Awaya (1988) showed that the Stokes layer separates periodically near a breaking point when two-dimensional regular waves climb up a sloping flat bed, and that the separated flow forms a vortical pattern and lifts up a large amount of sediment.

On the other hand, the fluid motion is usually considered to be irrotational in the offshore zone. The Lagrangian mass transport of fluid in waves is one of interesting problems in this zone. Bagnold (1947) carried out experiments in which two-dimensional regular waves propagated on a horizontal smooth bed. He found a strong forward drift current along the bed, and a weak backward one induced under the water surface. The difference between Bagnold's observation and the well-known 'Stokes drift' created a sensation. Longuet-Higgins (1953) solved this problem theoretically by taking into account the existence of the Stokes layer. Russell & Osorio (1958) measured the forward drift velocities at the outside edge of the Stokes layer for horizontal, up-sloping and down-sloping beds. Their data collapse well onto the theoretical curve

obtained by Longuet-Higgins. Those authors also carried out laboratory experiments to confirm Bagnold's results in the case when two-dimensional regular waves climb up a sloping bed. At that time, they found a row of vortices forming under the waves. As stated previously, the fluid motion in the offshore zone has been treated generally as irrotational. Therefore, this is a fresh phenomenon in fluid dynamics as well as coastal engineering.

In this paper, the qualitative and quantitative properties of this vortex train are investigated experimentally.

2. Experimental set-up and procedure

Figure 1 shows schematically the experimental apparatus. The wave tank was 12 m long, 0.4 m deep and 0.15 m wide. It was made of transparent acrylic plates and equipped with a sloping flat bed. The gradients of $\tan\theta = 1/37.0$, $1/23.5$ and $1/12.3$ were used as bed slopes. Two-dimensional regular waves were made by oscillating a flap. The wave period T was varied from 0.517 s to 2.59 s. The wavelength in deep water L_0, calculated from $gT^2/2\pi$, was in the range from 0.417 m to 10.5 m, where g is the gravitational acceleration. The local wave height H was measured by using a capacitance-type wave gauge. The local wave velocity C was calculated from the time lag of the signals from two wave gauges which were set 20 cm apart. The wave height in deep water H_0 was evaluated by dividing the shoaling coefficient into H. The value of H_0 ranged from 0.93 cm to 6.58 cm. The local wavelength L was calculated from $L = CT$. These local quantities H, L and C and the local mean water depth h were measured at each position where the formation or non-formation of the vortices was confirmed or where the properties were measured.

Drift currents induced on the offshore side of the breaking point were observed by means of flow visualization. Granules of water-soluble aniline blue were used as a tracer. The granules scattered on the water surface of the offshore zone sink and form vertical dye lines. Typical flow patterns generated under the hydraulic conditions of $T = 1.06$ s, $L_0 = 1.75$ m, $H_0 = 3.6$ cm and $\tan\theta = 1/23.5$ were photographed through a sidewall of the tank using a 35 mm camera. The camera was at rest with respect to the tank. The direction of wave propagation is from right to left in all the photos presented below. Whether a vortex train formed or not was confirmed visually. The behaviour of vortices was videotaped to evaluate their characteristic quantities, i.e. the horizontal lengthscale of the vortices l and the velocity of vortex movement u. The lengthscale, which is defined by the horizontal distance from centre to centre, was determined by sampling dozens of pictures in which the vortices form a regular pattern over a distance of 0.5 m (e.g. see figures 3*b* and 3*c*), and by averaging the vortex spacings read from the pictures over a number of samples. About ten sampled pictures were used for the evaluation of each value of u. The value of u was obtained by dividing a given distance by the time taken for a vortex to move through the distance, and by averaging the velocities measured in this way over the sampling number.

3. Qualitative properties of the offshore vortex train

Figure 2(*a–d*) shows the deformation of lines of dye, which were formed due to the settling of granules of aniline blue scattered on the water surface between positions C and B. The lines can be called time lines. The time elapsed after the scattering is denoted by t. As observed by Bagnold, figures 2(*a*) and 2(*b*) show a strong onshore drift current to be induced along the sloping bed and a weak offshore one to form

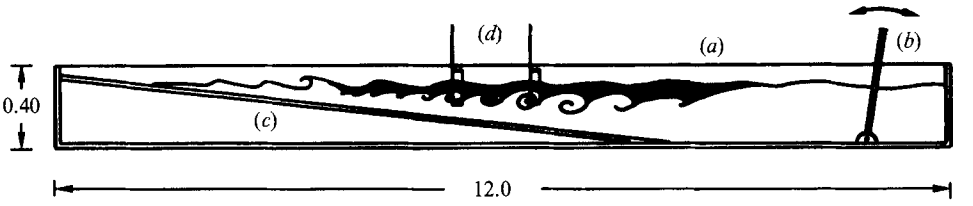

FIGURE 1. Schematic diagram of experimental set-up (dimensions in m): (*a*) tank; (*b*) wave maker; (*c*) sloping bed; (*d*) wave gauges.

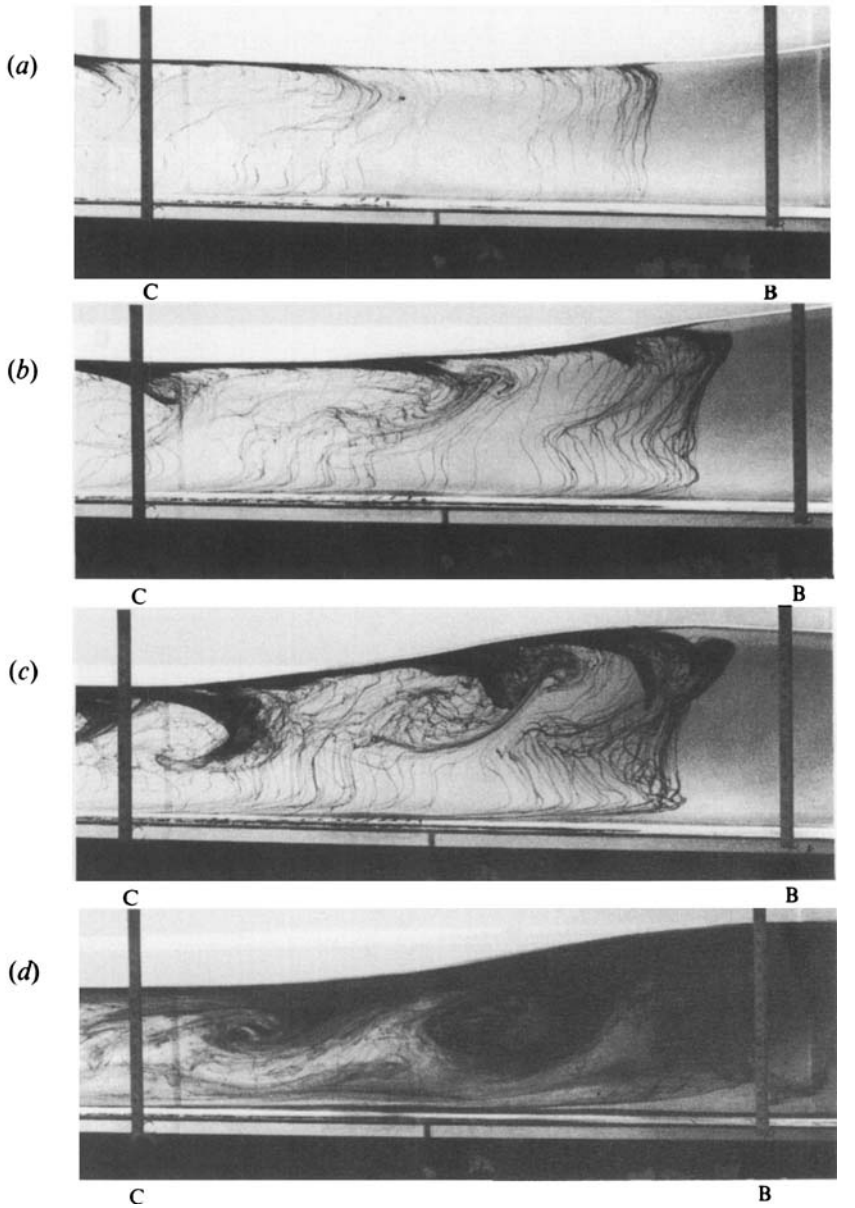

FIGURE 2. Deformation of time lines. The distance between C and B is 0.5 m. (*a*) $t/T = 2.83$; (*b*) 24.5; (*c*) 40.6; (*d*) 170.

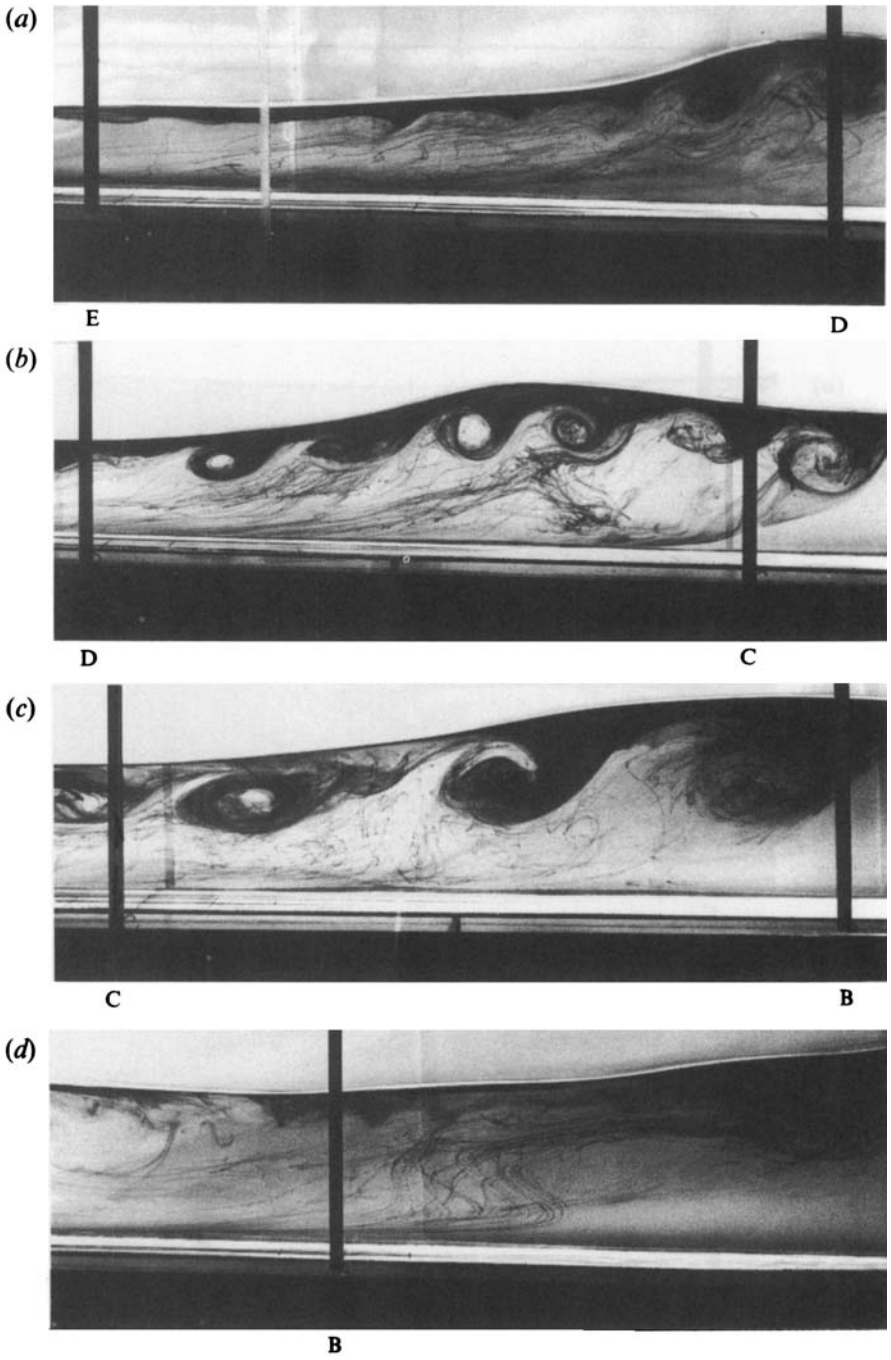

FIGURE 3. Patterns of vortex trains in the offshore direction. Mean water depth is 7.9 cm at E, 10 cm at D, 12 cm at C and 14 cm at B.

under the water surface. The time lines shown in figure 2(*c*) form a vortical pattern with clockwise rotation. This indicates the existence of vorticity along the water surface of the offshore zone. A row of vortices forming a regular pattern between C and B is seen in figure 2(*d*). Its formation seems to be due to the shear instability between the

onshore drift current and the offshore one. In this paper, hereafter, let us call it the offshore vortex train.

Figure 3(*a–d*) shows a variation in the pattern of the vortex train in the offshore direction. The distances between positions E, D, C and B are 0.5 m, respectively. The breaking point was 0.68 m shoreward from E. The wavy pattern of dye seen in figure 3(*a*) may indicate the onset of the instability. It develops into large vortical rollers between D and B. The distance between the vortices increases with the water depth. As shown in figure 3(*d*), however, the vortical pattern disappears in the region offshore from B. The decay of vortices may be caused by the decrease of shear strain rate between the two drift currents.

Figure 4(*a–f*) shows the merging of the offshore vortices. Here, t is the time elapsed from when the photograph of figure 4(*a*) was taken. Let us follow the two vortices indicated by the arrows. Moving in the offshore direction, they gradually approach each other as shown in figure 4(*b–e*), and merge into one vortex as shown in figure 4(*f*). In this way, the offshore vortices adjust their distance apart and keep them at the order of magnitude of the water depth.

4. Formation region of the vortex train

Figure 5 shows the relation between the formation of the offshore vortex train and the types of breaking waves. The open and solid circles indicate its formation and non-formation, respectively. The two solid lines are border lines between three types of breakers, which are given by Gaughan & Komar (1975). It is seen from this figure that whether the vortex train forms or not is separated by the dash-dot line, i.e. $H_0/L_0 = 4.2 \times 10^{-2}$, and that it is independent of the breaker type.

The region in which the vortices are observed can be determined in terms of the variables h, L, H, T, c, g and $\tan\theta$. Two variables can be eliminated by taking into account the dispersion relation of water waves and the relation $C = L/T$. If C and g are chosen as the two variables and a dimensional analysis is performed, a non-dimensional expression for the formation region is given by

$$f(H/L, h/L, \tan\theta). \tag{1}$$

In figure 6(*a–c*), the regions of vortex formation and non-formation are indicated by the open and solid circles, respectively. The solid curves show the limiting wave steepness. This figure make it clear that the offshore vortices form in a shallow region offshoreward from the breaking point when the wave steepness is relatively small. The reason for this may be that at a large wave steepness, an onshoreward drift current forms near the water surface because the well-known Stokes drift overcomes the offshoreward drift current.

Let us try to represent the three formation regions shown in figure 6(*a–c*) in a uniform manner. For this purpose a coordinate system should be chosen that unifies the curves of limiting wave steepness. Various empirical relations between the wavelength L_b, wave height H_b and water depth h_b at the breaking point have been proposed (e.g. McCowan 1894 and Miche 1944). Galvin (1972) gives a relation including the bed slope:

$$H_b/L_b = 0.72(1 + 6.4\tan\theta)\, h_b/L_b. \tag{2}$$

In figure 7, the data obtained in this study are plotted to confirm the validity of Galvin's relation. The measured values for $\tan\theta = 1/10$ are also included in this figure. The solid line is obtained by applying the least-squares method to these data. Though

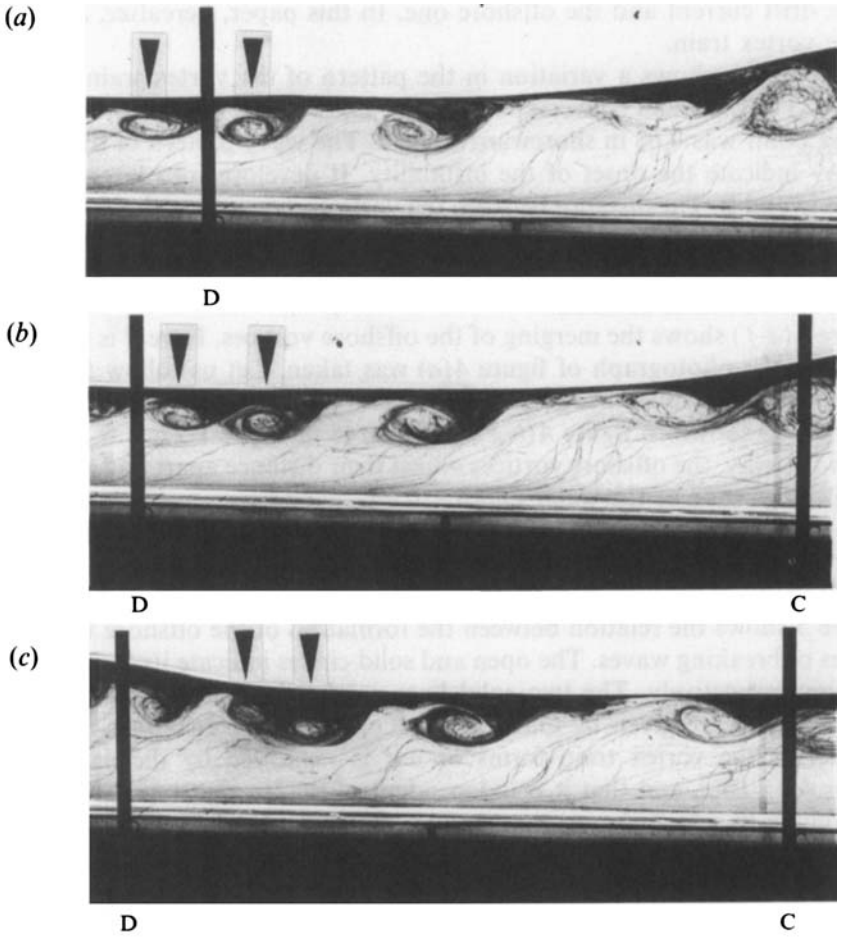

FIGURE 4 (*a–c*). For caption see facing page.

the data agree well with relation (2) at $H_b/L_b \leqslant 0.05$, the agreement becomes much worse in the range of $H_b/L_b > 0.05$. However, it is important that the limit of wave steepness over the wide range of H_b/L_b can be expressed by using this coordinate system.

In figure 8, the data shown in figure 6(*a–c*) are replotted in the coordinate system of H/L and $(1+6.4\tan\theta)h/L$. The three formation regions are unified in the region bounded by three solid lines (*a*), (*b*) and (*c*). The offshore vortices form when waves with $H_0/L_0 \leqslant 4.2\times10^{-2}$ propagate on a sloping bed. The onshore border of vortex formation is the breaking point, and that of the offshore side is given by line (*c*).

5. Quantitative properties

5.1. *Horizontal lengthscale of offshore vortices*

The horizontal distance between offshore vortices l can be described completely by using the seven characteristic parameters h, L, H, C, T, g and $\tan\theta$. As discussed in §4, however, two dimensional parameters can be removed from these seven. If C and g are eliminated, a dimensionless form of l is given by

$$l/h = f(H/L, h/L, \tan\theta). \tag{3}$$

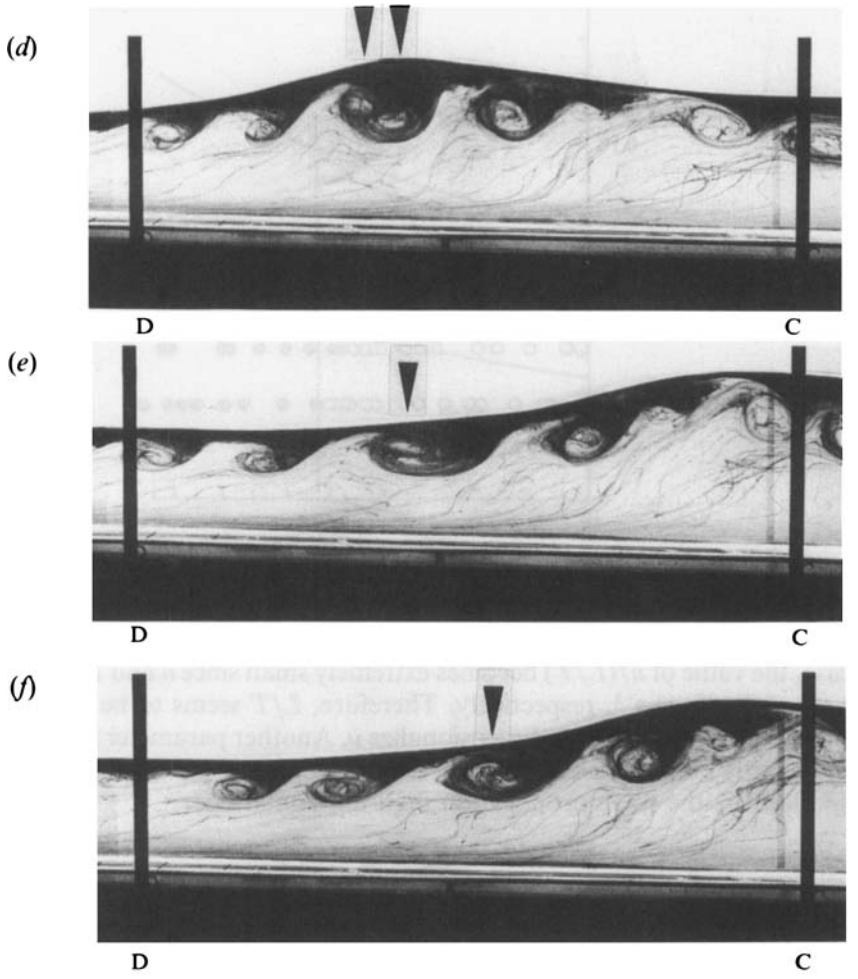

FIGURE 4. Merging of offshore vortices. (*a*) $t/T = 0$; (*b*) 12.3; (*c*) 23.0; (*d*) 25.5; (*e*) 30.1; (*f*) 37.7.

Plotting the measured values of l/h for each value of $\tan\theta$ against H/L, we obtained the result that l/h is proportional to $(H/L)^{-1}$, but no systematic dependence of l/h on h/L was seen. Furthermore, we found the ratio $(l/h)/(H/L)^{-1}$ to be approximately proportional to $(\tan\theta)^{-1/3}$. From these results, an empirical relation for the vortex spacing is given by

$$l/h = 1.2 \times 10^{-2}(\tan\theta)^{-1/3}(H/L)^{-1}. \tag{4}$$

A comparison of the experimental data and equation (4) is shown in figure 9. It is seen that the data collapse well onto the empirical line. Another important feature is that l/h is of order of magnitude of unity. This means that the lengthscale of the offshore vortices is controlled mainly by the local water depth.

5.2. *Velocity of vortex movement*

The offshore vortices move slowly in the offshore direction. As discussed above, their velocity u also depends on h, L, H, T and $\tan\theta$. Dimensional considerations give

$$u/(L/T) = f(h/L, H/L, \tan\theta). \tag{5}$$

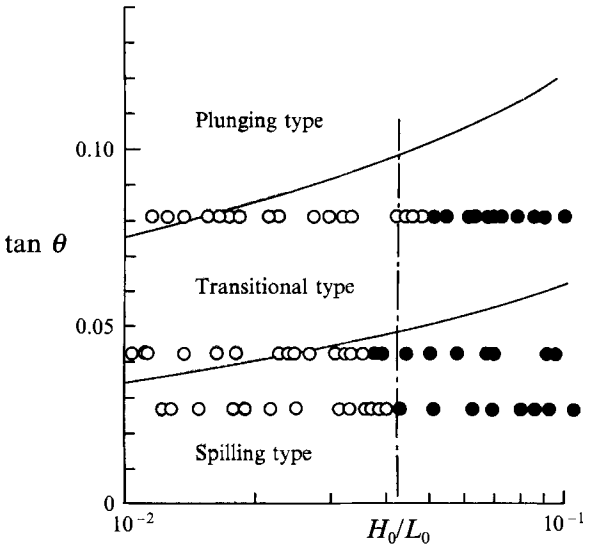

FIGURE 5. Relation between the formation of vortices and the types of breaking: ○, formation of offshore vortex train; ●, non-formation.

In this case, the value of $u/(L/T)$ becomes extremely small since u and L/T are of order 10^{-1} cm s^{-1} and 10^{2} cm s^{-1}, respectively. Therefore, L/T seems to be unsuitable as a representative parameter to non-dimensionalize u. Another parameter is the velocity of the offshore drift current in the offshore zone. Longuet-Higgins derived its velocity profile induced by the wave propagation on a horizontal bed,

$$U(z) = (\pi H/L)^2 \, CF(z/h), \tag{6}$$

where

$$F(\mu) = \frac{-1}{4\sinh^2 kh}\Big[2\cosh\{2kh(\mu-1)\}+3+kh\sinh\{2kh(3\mu^2-4\mu+1)\} + 3\left(\frac{\sinh 2kh}{2kh}+\frac{3}{2}\right)(\mu^2-1)\Big]; \tag{7}$$

the z-axis is taken in the direction downward from the mean water level and k is the wavenumber. A positive value of $F(\mu)$ means that $U(z)$ is in the offshore direction. The vertical profile given by (7) takes a positive maximum value F_{max}, and F_{max} decreases monotonically with the increase of kh. Here, let us introduce the maximum offshore velocity calculated from

$$U_{max} = (\pi H/L)^2 \, CF_{max} \tag{8}$$

as a representative parameter controlling u. In this case, a dimensionless form is given by

$$u/U_{max} = f(h/L, H/L, \tan\theta). \tag{9}$$

Plotting the measured values of u/U_{max} against h/L for three bed slopes, we found a tendency for u/U_{max} to increase in proportion to h/L and no systematic dependence of u/U_{max} on H/L is seen. We found also the ratio $(u/U_{max})/(h/L)$ to depend on $(\tan\theta)^{2/3}$. From these results, an empirical relation for the velocity of vortex movement,

$$u/U_{max} = 3.6\times 10^{1}(\tan\theta)^{2/3}(h/L) \tag{10}$$

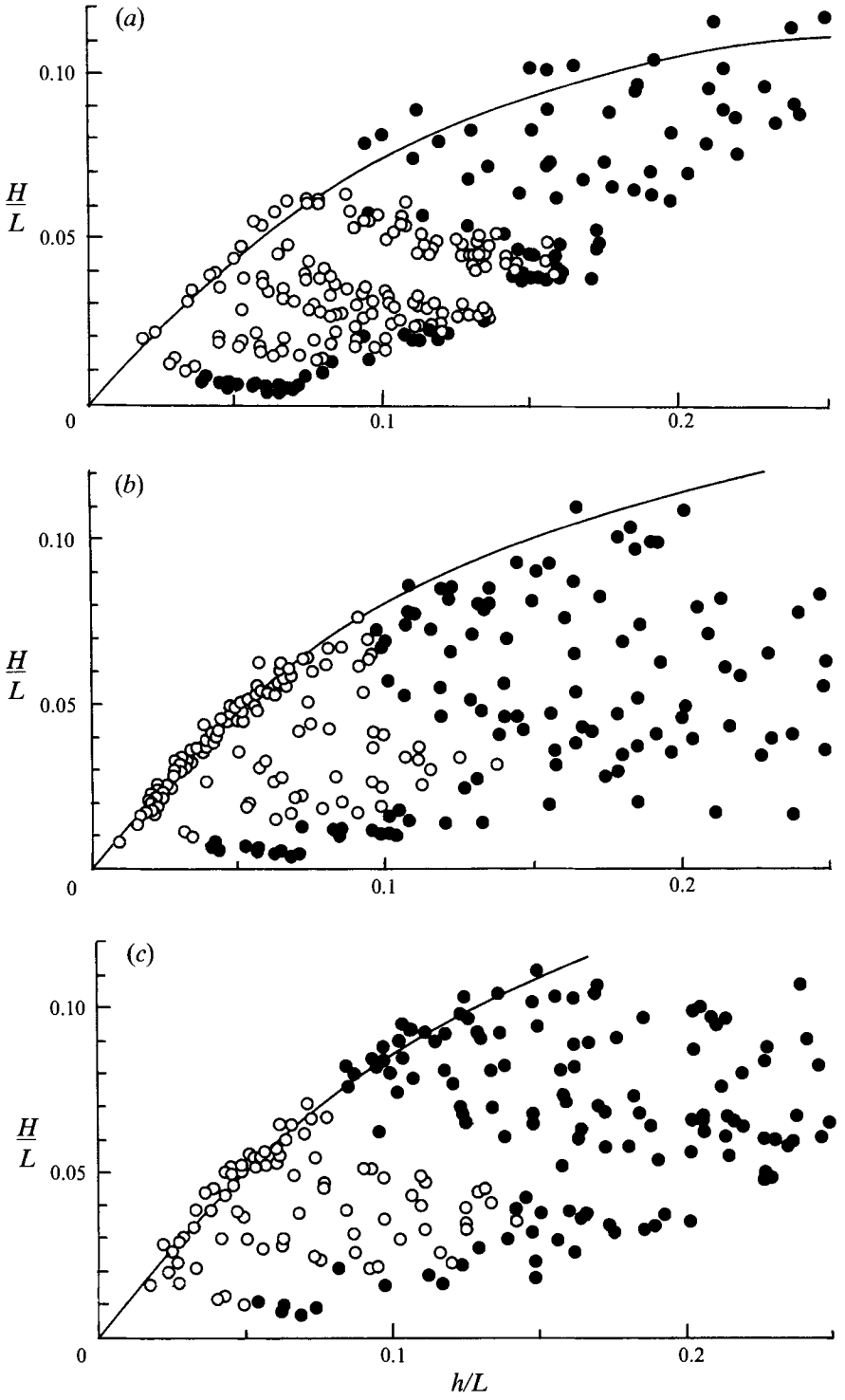

FIGURE 6. Formation regions of offshore vortices. (*a*) $\tan\theta = 1/37.0$; (*b*) 1.23.5; (*c*) 1/12.3. ○, Formation of offshore vortex train; ●, non-formation.

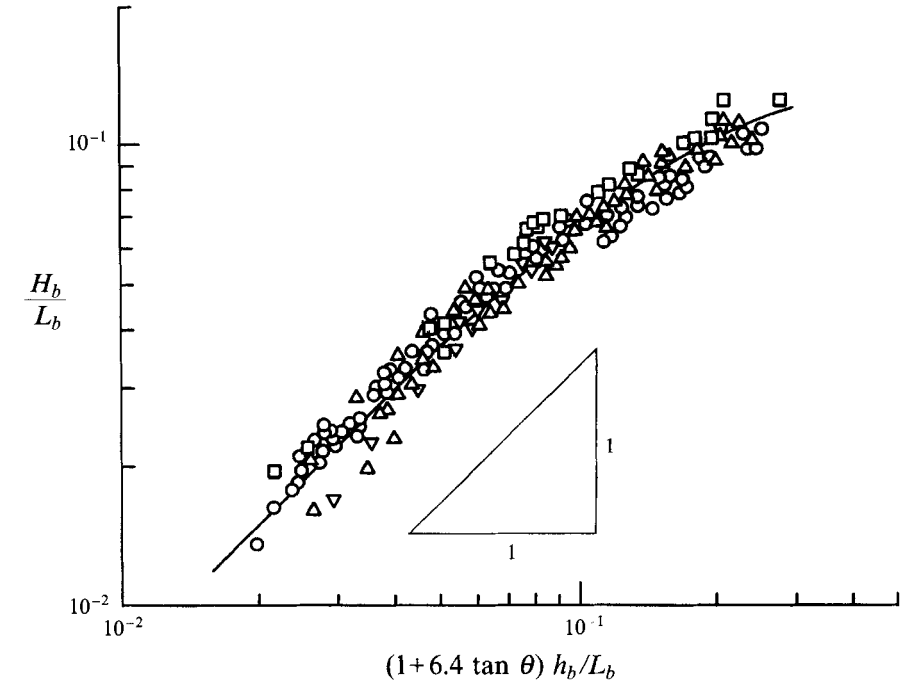

FIGURE 7. Relation between characteristic quantities at the breaking point: □, $\tan\theta = 1/37.0$; ○, 1/23.5; △, 1/12.3; ▽, 1/10.0.

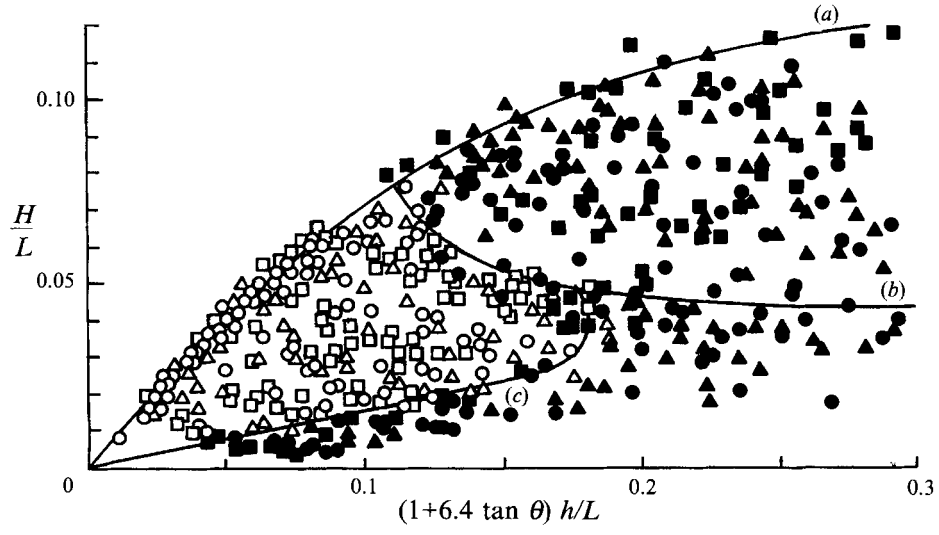

FIGURE 8. Unified formation region of offshore vortices: open symbols, formation of offshore vortex; solid symbols, non-formation. □, ■, $\tan\theta = 1/37.0$; ○, ●, 1/23.5; △, ▲, 1/12.3. Lines (*a*) and (*b*) indicate the limit of wave steepness and $H_0/L_0 = 4.2 \times 10^{-2}$, respectively. Line (*c*) is the offshore border of vortex formation.

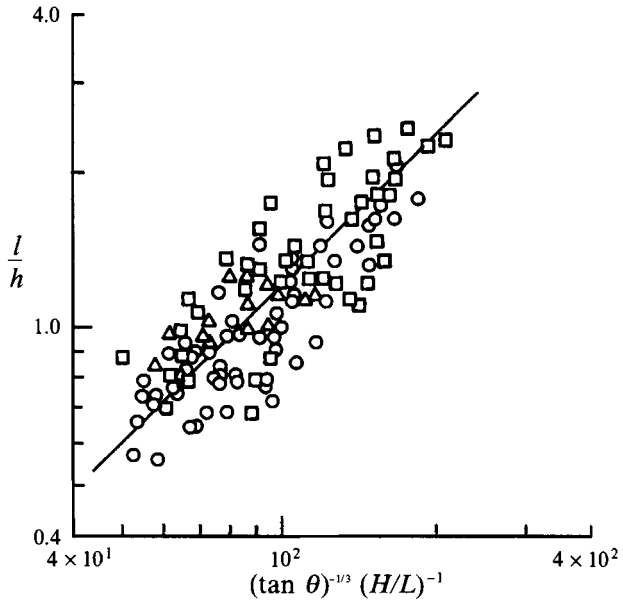

FIGURE 9. Empirical relation for vortex spacing: □, $\tan\theta = 1/37.0$; ○, 1/23.5; △, 1/12.3.

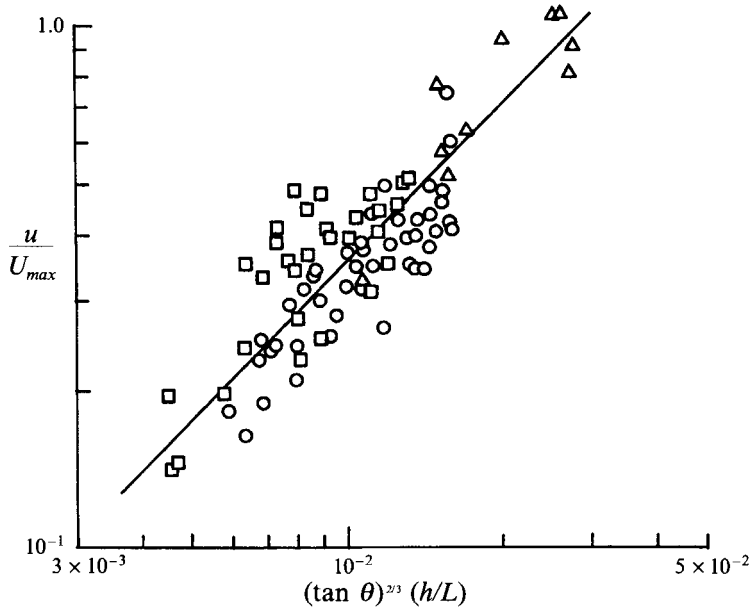

FIGURE 10. Empirical relation for the velocity of vortex movement: □, $\tan\theta = 1/37.0$; ○, 1/23.5; △, 1/12.3.

is obtained. A comparison of the experimental data and (10) is made in figure 10. Good agreement is seen.

6. Conclusions

It was found that a row of vortices, which was called the offshore vortex train, forms along the water surface of an offshore zone when two-dimensional regular waves whose

steepness in deep water is smaller than 4.2×10^{-2} run up a sloping bed. This seems to occur owing to the shear instability between the onshore drift current and the offshore one. The instability starts near the breaking point. Moving in the offshore direction, the vortices merge with each other and increase their spacing at the order of magnitude of water depth. After reaching a particular offshore location, they begin to decay because of the decrease of the strain rate between the two drift currents. Universal empirical expressions were obtained for the formation region of the offshore vortices, their horizontal lengthscales and the velocities of vortex movement.

The authors wish to thank Professors H. Honji and T. Komatsu for stimulating discussions and Mrs Arizumi for her help in the preparation of the manuscript.

REFERENCES

BAGNOLD, R. A. 1947 Sand movement by waves: some small-scale experiments with sand of very low density. *J. Inst. Civil Engrs* **27**, 447–469.

BATTJES, J. A. 1988 Surf-zone dynamics. *Ann. Rev. Fluid Mech.* **20**, 257–293.

GALVIN, C. J. 1972 Wave breking in shallow water. In *Waves on Beaches* (ed. R. E. Meyer), pp. 413–456. Academic.

GAUGHAN, M. K. & KOMAR, P. D. 1975 The theory of wave propagation in water of gradually varying depth, and the prediction of breaker type and height. *J. Geophys. Res.* **80**, 2991–2996.

KOMAR, P. D. 1976 *Beach Processes and Sedimentation*, pp. 11–13. Prentice-Hall.

LONGUET-HIGGINS, M. S. 1953 Mass transport in water waves. *Phil. Trans. R. Soc. Lond.* A **245**, 535–581.

MATSUNAGA, N. & HONJI, H. 1980 The backwash vortex. *J. Fluid Mech.* **99**, 813–815.

MATSUNAGA, N., TAKEHARA, K. & AWAYA, Y. 1988 Coherent eddies induced by breakers on a sloping bed. *Proc. 21st Conf. on Coastal Engng*, pp. 234–245. ASCE.

MCCOWAN, M. A. 1894 On the highest wave of permanent type. *Phil. Mag.* (5) **38**, 351–357.

MICHE, R. 1944 Mouvements ondulatoires de la mersen profondeur constante ou decroissante. *Ann. Ponts Chaussees* **114**, 369–406.

MILLER, R. L. 1976 Role of vortices in surf zone prediction: sedimentation and wave forces. *Beach and Nearshore Sedimentation, SEPM Spec. Pub.* vol. 23, pp. 92–114.

PEREGRINE, D. H. 1983 Breaking waves on beaches. *Ann. Rev. Fluid Mech.* **15**, 149–178.

RUSSELL, R. C. H. & OSORIO, D. C. 1958 An experimental investigation of drift profiles a closed channel. *Proc. 6th Conf. on Coastal Engng*, pp. 171–183. ASCE.